



# Synthesis and enzymatic ketonization of the 5-(halo)-2-hydroxy-2,4-pentadienoates and 5-(halo)-2-hydroxy-2,4-pentadienoates

Tyler M. M. Stack<sup>1</sup>, William H. Johnson Jr.<sup>2</sup> and Christian P. Whitman<sup>\*2</sup>

## Full Research Paper

Open Access

### Address:

<sup>1</sup>Department of Molecular Biosciences, College of Natural Sciences, 1 University Station, University of Texas, Austin, TX 78712, USA and <sup>2</sup>Division of Chemical Biology and Medicinal Chemistry, College of Pharmacy, 1 University Station, University of Texas, Austin, TX 78712, USA

### Email:

Christian P. Whitman\* - whitman@austin.utexas.edu

\* Corresponding author

### Keywords:

dienol; enzyme kinetics; fluoride; halogen

*Beilstein J. Org. Chem.* **2017**, *13*, 1022–1031.

doi:10.3762/bjoc.13.101

Received: 19 March 2017

Accepted: 11 May 2017

Published: 26 May 2017

Associate Editor: K. N. Allen

© 2017 Stack et al.; licensee Beilstein-Institut.

License and terms: see end of document.

## Abstract

5-Halo-2-hydroxy-2,4-pentadienoates and 5-halo-2-hydroxy-2,4-pentadienoates are stable dienols that are proposed intermediates in bacterial *meta*-fission pathways for the degradation of halogenated aromatic compounds. The presence of the halogen raises questions about how the bulk and/or electronegativity of these substrates would affect enzyme catalysis or whether some pathway enzymes have evolved to accommodate it. To address these questions, 5-halo-2-hydroxy-2,4-pentadienoates (5-halo = Cl, Br, F) were synthesized and a preliminary analysis of their enzymatic properties carried out. In aqueous buffer, 5-halo-2-hydroxy-2,4-pentadienoates rapidly equilibrate with the  $\beta,\gamma$ -unsaturated ketones. For the 5-chloro and 5-bromo derivatives, a slower conversion to the  $\alpha,\beta$ -isomers follows. There is no detectable formation of the  $\alpha,\beta$ -isomer for the 5-fluoro derivative. Kinetic parameters were also obtained for both sets of compounds in the presence of 4-oxalocrotonate tautomerase (4-OT) from *Pseudomonas putida* mt-2 and *Leptothrix cholodnii* SP-6. For 5-halo-2-hydroxy-2,4-pentadienoates, there are no major differences in the kinetic parameters for the two enzymes (following the formation of the  $\beta,\gamma$ -unsaturated ketones). In contrast, the *L. cholodnii* SP-6 4-OT is  $\approx 10$ -fold less efficient than the *P. putida* mt-2 4-OT in the formation of the  $\beta,\gamma$ -unsaturated ketones and the  $\alpha,\beta$ -isomers from the 5-halo-2-hydroxy-2,4-pentadienoates. The implications of these findings are discussed. The availability of these compounds will facilitate future studies of the haloaromatic catabolic pathways.

## Introduction

Aromatic hydrocarbons and their halogenated derivatives are well known environmental contaminants [1-5]. Halogenated aromatic compounds are found in many industrial commodities such as pesticides, flame-retardants, hydraulic fluids, and synthetic intermediates for pharmaceutical agents [2-4]. Several

strategies are being explored to remove these toxic compounds from the environment. One particularly attractive strategy is bioremediation, which uses microbial catabolic pathways to process the toxic species to metabolic intermediates that frequently can be channeled to the Krebs Cycle [2-5]. This ap-

proach requires a thorough understanding of each of the pathway steps. This information is also useful to predict the fate of halogenated species once released into the environment.

One major route for the degradation of aromatic compounds is the *meta*-fission pathway [6,7]. The enzymes and reactions of the *meta*-fission pathway in *Pseudomonas putida* mt-2 for monocyclic aromatic compounds (e.g., benzene, toluene, and alkyl-substituted derivatives) have been extensively studied for more than 60 years. Initially, the aromatic compound is converted to catechol or a catechol derivative. Subsequently, the resulting species undergoes *meta*-fission where this term refers to the position of the ring fission (shown on **1** in Scheme 1). An extradiol dioxygenase processes catechol **1** to 2-hydroxymuconate semialdehyde **2**, which is oxidized by an NAD<sup>+</sup>-dependent dehydrogenase to yield 2-hydroxymuconate (**3a**) [6,7]. Ketonization of **3a** to 2-oxo-3-hexenedioate (**4a**) is catalyzed by 4-oxalocrotonate tautomerase (4-OT) [8]. Decarboxylation of **4a** by the metal-dependent 4-oxalocrotonate decarboxylase (4-OD) generates 2-hydroxy-2,4-pentadienoate (**5a**) [9–11]. 4-OD functions in a complex with the next enzyme in the pathway, a metal-dependent vinylpyruvate hydratase (VPH) [7]. VPH catalyzes the addition of water to the C-4 position of **5a** to produce (*S*)-2-keto-4-hydroxypentanoate (**6a**) [9–11]. A retroaldol cleavage of **6a** by pyruvate aldolase yields pyruvate and acetaldehyde (**7a**). Pyruvate aldolase is tightly coupled with an acetaldehyde dehydrogenase, which uses NAD<sup>+</sup> and coenzyme A to produce acetyl-CoA (**8a**) [12]. Pyruvate and acetyl-CoA can then be funneled into the Krebs cycle.

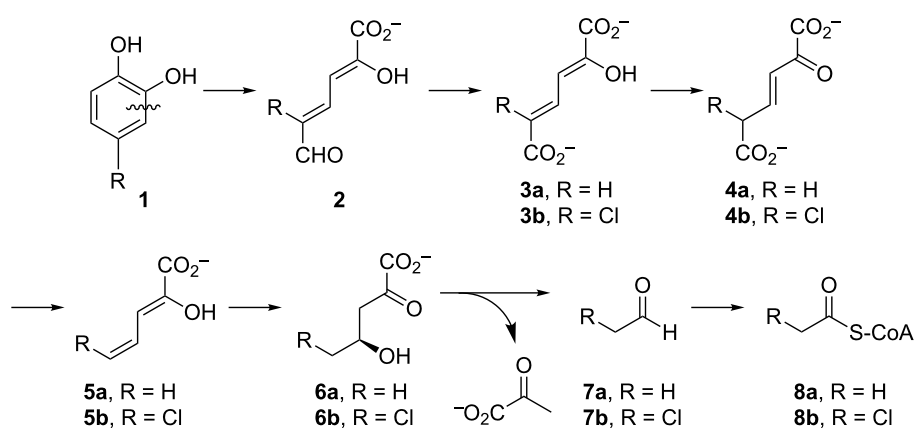
Over the years, variations of this pathway have been reported that process halogenated catechols. One such pathway is found in *Comamonas* sp. strain CNB-1, which grows on 4-chloronitro-

benzene as a sole carbon and energy source [3,13]. The reported pathway shows the chloro substituent at the C5 position to produce **3b–6b** (Scheme 1), but there is little chemical proof for the structures. In addition, if the proposed pathway in *C. sp.* strain CNB-1 follows that of the canonical one, then the actions of pyruvate aldolase and acetaldehyde dehydrogenase would produce 2-chloroacetaldehyde (**7b**) and 2-chloroacetyl CoA (**8b**), which are potential alkylating agents of these enzymes as well as other cellular proteins and DNA. This observation and the potential effects of the halogen on other enzyme-catalyzed steps in the pathway suggest that these enzymes might have evolved strategies to accommodate the halogen that mitigate potentially harmful consequences [4]. To explore these possibilities and the consequences of halogen substitution, a series of compounds were synthesized (**3b–d** and **5b–d**, Scheme 2) and a preliminary analysis of their properties carried out. The results are reported herein.

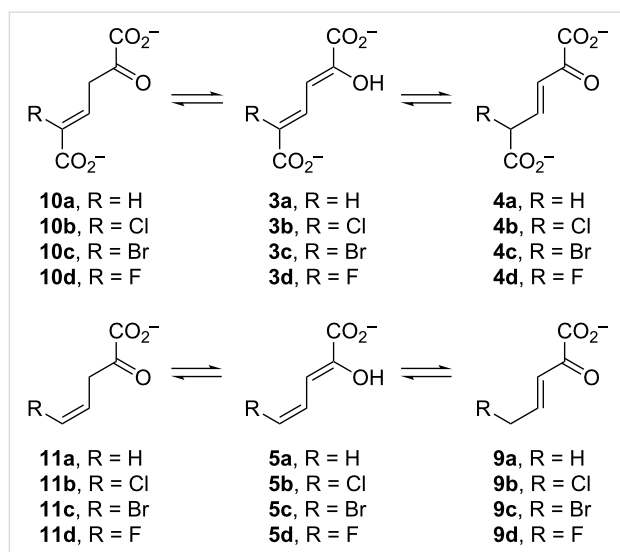
## Results and Discussion

### Synthesis of **3c,d** and **5c,d**

The 5-bromo- and 5-fluoro-2-hydroxymuconates (**3c** and **3d**) were successfully synthesized following the protocol used elsewhere to generate 5-chloro-2-hydroxymuconate (**3b**) [11]. These reactions combine the ethyl 2-halocrotonate with diethyl oxalate followed by alkaline hydrolysis and acidification. Subsequently, the 4*Z*-isomers of 5-bromo- and 5-fluoro-2-hydroxy-2,4-pentadienoates (**5c** and **5d**) were synthesized enzymatically (following the protocol for the 5-chloro derivative). The enzymatic synthesis relies on the actions of the 4-OT and 4-OD/E106QVPH (both from *P. putida* mt-2), which carry out ketonization and decarboxylation, respectively, of **3c** and **3d** [11]. (The 4-OD/E106QVPH retains full decarboxylase activity, but has very little hydratase activity [10].) The observation that



**Scheme 1:** The *meta*-fission pathway in *P. putida* mt-2 and *Comamonas* sp. strain CNB-1. The degradation of toluene generates the intermediates where R = H (compounds **3a–8a**). The degradation of 4-chloronitrobenzene in *C. sp.* strain CNB-1 is proposed to use similar enzymatic steps where R = Cl (compounds **3b–8b**).



**Scheme 2:** The ketonization of dienols **3** and **5**, to the corresponding  $\alpha,\beta$ -unsaturated ketones (**4** and **9**, respectively) and the  $\beta,\gamma$ -unsaturated ketones (**10** and **11**, respectively).

this protocol generates the 4Z-isomers of **5b–d** indicates that the halogen does not affect the stereochemical outcome of the 4-OD-catalyzed reaction.

In the course of these experiments, it was observed that the generation of **5d** required the addition of 4-OT every minute over a 40 min period, whereas the generation of **5b,c** did not. Analysis of the reactions showed that all three resulted in the irreversible inactivation of 4-OT, but **5d** is the most potent. The full analysis and implications of these findings will be reported in the near future. However, these findings prompted us to investigate

the 4-OT-catalyzed ketonization of these dienols, especially **5b–d**.

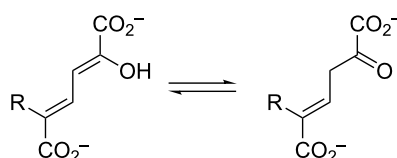
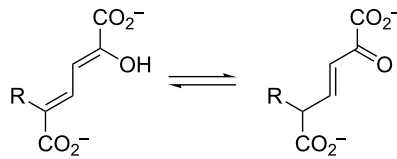
### Ketonization of **3a–d** by Pp and Lc 4-OTs

We have previously shown that *P. putida* mt-2 4-OT rapidly converts **3a** to  $\beta,\gamma$ -unsaturated ketone **10a** before a slower conversion to the  $\alpha,\beta$ -unsaturated isomer **4a** [8]. Isomer **4a** is the thermodynamically stable one ( $\approx 80\%$  at equilibrium) and the substrate for 4-OD, which is the next enzyme in the pathway (Scheme 1). The kinetic analysis for the ketonization of **3b–d** to **4b–d** is complicated by the much lower amounts of the  $\alpha,\beta$ -unsaturated ketones present at equilibrium and the faster conversion of the dienols to the  $\beta,\gamma$ -unsaturated ketones [14]. Hence, we only examined the ketonization of the dienols to the  $\beta,\gamma$ -unsaturated ketones (following the loss of the  $\lambda_{\max}$  associated with the dienol).

The steady-state kinetic parameters for the 4-OT-catalyzed ketonization of **3b–d** (to **10b–d**) were determined with the enzymes from *P. putida* mt-2 and *L. cholodnii* SP-6. 4-OT from *P. putida* mt-2 (designated Pp 4-OT) represents the canonical *meta*-fission pathway and 4-OT from *L. cholodnii* SP-6 (designated Lc 4-OT) represents the haloaromatic *meta*-fission pathway. The Lc 4-OT shows high similarity (78% identity and 87% similarity) with the one found in *Comamonas* sp. strain CNB-1, which is not available [11]. The Lc 4-OT is more distantly related to the Pp 4-OT (45% identity and 71% similarity).

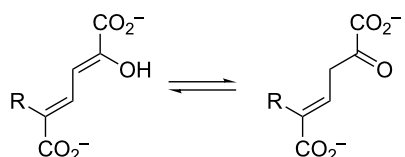
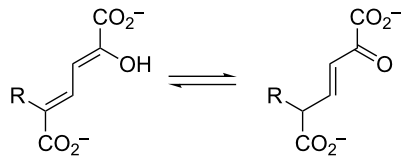
The kinetic parameters are shown in Table 1 and Table 2. The kinetic parameters are comparable for two enzymes. For the Pp

**Table 1:** Kinetic parameters for Pp 4-OT using **3a–d**.<sup>a</sup>

| Reaction  | $k_{\text{cat}}$ (s <sup>-1</sup> )              | $K_m$ ( $\mu\text{M}$ )                     | $k_{\text{cat}}/K_m$ (M <sup>-1</sup> s <sup>-1</sup> )                                       |
|---|--|---|---|
| <br><b>3b</b> : R = Cl <b>10b</b> : R = Cl<br><b>3c</b> : R = Br <b>10c</b> : R = Br<br><b>3d</b> : R = F <b>10d</b> : R = F | <br>220 $\pm$ 10<br>210 $\pm$ 10<br>630 $\pm$ 30 | <br>60 $\pm$ 10<br>32 $\pm$ 3<br>34 $\pm$ 4 | <br>3.8 $\pm$ 0.7 $\times 10^6$<br>6.6 $\pm$ 0.7 $\times 10^6$<br>1.9 $\pm$ 0.2 $\times 10^7$ |
| <br><b>3a</b> : R = H <b>4a</b> : R = H  | 2100 $\pm$ 100                                   | 100 $\pm$ 10                                | 2.1 $\pm$ 0.2 $\times 10^7$   |

<sup>a</sup>The steady-state kinetic parameters were determined under the conditions described in the text. Errors are standard deviations.

**Table 2:** Kinetic parameters for Lc 4-OT using **3a–d**.<sup>a</sup>

| Reaction  |                    | $k_{\text{cat}}$ (s <sup>-1</sup> ) | $K_{\text{m}}$ (μM) | $k_{\text{cat}}/K_{\text{m}}$ (M <sup>-1</sup> s <sup>-1</sup> ) |
|---|--------------------|-------------------------------------|---------------------|--|
|  |                    |                                     |                     |  |
| <b>3b:</b> R = Cl   | <b>10b:</b> R = Cl | 350 ± 20                            | 60 ± 10             | 5.8 ± 1.0 × 10 <sup>6</sup>                                      |
| <b>3c:</b> R = Br   | <b>10c:</b> R = Br | 420 ± 40                            | 60 ± 10             | 7.0 ± 1.0 × 10 <sup>6</sup>                                      |
| <b>3d:</b> R = F  | <b>10d:</b> R = F  | 420 ± 40                            | 40 ± 10             | 1.1 ± 0.3 × 10 <sup>7</sup>                                      |
|  |                    |                                     |                     |  |
| <b>3a:</b> R = H  | <b>4a:</b> R = H   | 2400 ± 100                          | 170 ± 20            | 1.4 ± 0.2 × 10 <sup>7</sup>                                      |

<sup>a</sup>The steady-state kinetic parameters were determined under the conditions described in the text. Errors are standard deviations.

4-OT, the  $k_{\text{cat}}/K_{\text{m}}$  values for the fluoro derivative are higher ( $\approx 3$ – $5$ -fold), mostly due to an increase in  $k_{\text{cat}}$ . For the Lc 4-OT, the  $k_{\text{cat}}/K_{\text{m}}$  values for the fluoro derivative are also higher, but not as high as those for the Pp enzyme. The kinetic parameters indicate that neither enzyme shows a preference for the halogenated compound and that this particular reaction is not affected by the presence of the halogen (although the ketonization of **3** to **10** is not the biological reaction). The “native” 4-OT activity (**3a** to **4a**) was measured for both enzymes and found to be comparable.

### Composition of the equilibrium mixture for **5b–d**

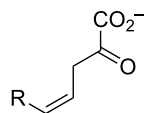
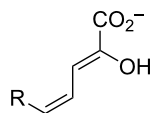
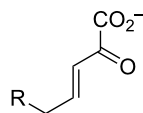
Dienols **5b–d** were allowed to equilibrate in 100 mM Na<sub>2</sub>HPO<sub>4</sub> buffer (final pH 6.8–7.2) in the presence of Pp 4-OT, and the identities of the components of the mixture were determined by <sup>1</sup>H NMR spectroscopy. The <sup>1</sup>H, <sup>13</sup>C, and <sup>19</sup>F NMR data are

presented in Supporting Information File 1. The approximate percentages of the components were determined by integration and are summarized in Table 3 [15]. The highly electronegative fluoride substituent in **5d** prevents the detectable formation of the corresponding  $\alpha,\beta$ -unsaturated ketone, **9d**.

### Ketonization of **3a–d** and **5a–d** by Pp and Lc 4-OT

Previous work has shown that 4-OT partitions a host of dienols to their  $\beta,\gamma$ - and  $\alpha,\beta$ -unsaturated ketones [16,17]. The behavior of **5b–d** is consistent with these observations. The steady state kinetic parameters for the Pp 4-OT-catalyzed conversion of **5b–d** to the  $\beta,\gamma$ -unsaturated ketones (**11b–d**, respectively) and  $\alpha,\beta$ -unsaturated ketones (**9b,c**, respectively) were determined, and compared to those for the non-halogenated species (**5a** to **11a** and **5a** to **9a**) (Table 4). For ketonization to the  $\beta,\gamma$ -unsaturated ketones, the  $k_{\text{cat}}/K_{\text{m}}$  values are comparable ranging from

**Table 3:** Equilibrium mixture of **5b–d**.

|        |  |  |  |
|--------|---|---|---|
| R = Cl | <b>11b</b> = 39%<br>(+7% hydrate) <sup>a</sup>                                      | <b>5b</b> = 15%   | <b>9b</b> = 39%   |
| R = Br | <b>11c</b> = 17%<br>(+13% hydrate) <sup>a</sup>                                     | <b>5c</b> = 9%  | <b>9c</b> = 61%   |
| R = F  | <b>11d</b> = 54%<br>(+22% hydrate) <sup>a</sup>                                     | <b>5d</b> = 24%   | N.D. <sup>b</sup>   |

<sup>a</sup>The hydrate of **11b–d** is present in varying amounts and depends on the halogen substitution. <sup>b</sup>N.D. not detected.

**Table 4:** Kinetic parameters for Pp 4-OT using **5a–d**.<sup>a</sup>

| Reaction          |                    | $k_{\text{cat}}$ (s <sup>-1</sup> ) | $K_{\text{m}}$ (μM) | $k_{\text{cat}}/K_{\text{m}}$ (M <sup>-1</sup> s <sup>-1</sup> ) |
|-------------------|--------------------|-------------------------------------|---------------------|--|
|                   |                    |                                     |                     |  |
| <b>5a:</b> R = H  | <b>9a:</b> R = H   | 2.9 ± 0.4                           | 1600 ± 250          | 1.8 ± 0.4 × 10 <sup>3</sup>                                      |
| <b>5b:</b> R = Cl | <b>9b:</b> R = Cl  | 0.5 ± 0.1                           | 1000 ± 250          | 5.0 ± 1.8 × 10 <sup>2</sup>                                      |
| <b>5c:</b> R = Br | <b>9c:</b> R = Br  | 1.7 ± 0.1                           | 320 ± 30            | 5.3 ± 0.6 × 10 <sup>3</sup>                                      |
|                   |                    |                                     |                     |  |
| <b>5a:</b> R = H  | <b>11a:</b> R = H  | 150 ± 16                            | 350 ± 50            | 4.3 ± 0.8 × 10 <sup>5</sup>                                      |
| <b>5b:</b> R = Cl | <b>11b:</b> R = Cl | 320 ± 25                            | 730 ± 87            | 4.4 ± 0.6 × 10 <sup>5</sup>                                      |
| <b>5c:</b> R = Br | <b>11c:</b> R = Br | 340 ± 11                            | 190 ± 12            | 1.8 ± 0.2 × 10 <sup>6</sup>                                      |
| <b>5d:</b> R = F  | <b>11d:</b> R = F  | 110 ± 10                            | 470 ± 56            | 2.3 ± 0.4 × 10 <sup>5</sup>                                      |

<sup>a</sup>The steady-state kinetic parameters were determined under the conditions described in the text. Errors are standard deviations.

2.3 × 10<sup>5</sup> (5-fluoro) to 1.8 × 10<sup>6</sup> M<sup>-1</sup> s<sup>-1</sup> (5-bromo) where the 5-bromo species has the highest value (4-fold higher than the non-halogenated species). For ketonization to the α,β-unsaturated ketones, the  $k_{\text{cat}}/K_{\text{m}}$  values are again comparable ranging from the 5.0 × 10<sup>2</sup> M<sup>-1</sup> s<sup>-1</sup> (5-chloro) to 5.3 × 10<sup>3</sup> M<sup>-1</sup> s<sup>-1</sup> (5-bromo). The α,β-unsaturated ketone **9d** (from **5d**) is not detectable (by UV or <sup>1</sup>H NMR spectroscopy).

The steady state kinetic parameters for the Lc 4-OT-catalyzed conversion of **5b–d** to the β,γ-unsaturated ketones (**11b–d**, respectively) were determined and compared to those for the non-halogenated species (**5a** to **11a**, Table 5). In all cases, the  $k_{\text{cat}}/K_{\text{m}}$  values are higher than that for **5a** ranging from 5.4–9.6-fold (for **5b** and **5c**, respectively). However, the values are lower than those determined for the Pp 4-OT-catalyzed reaction, ranging from 7.9–39-fold (for **5d** and **5c**, respectively).

The Lc 4-OT is not as efficient as the Pp 4-OT in generating the α,β-unsaturated ketones (**9a–c**) from the dienols (**5a–c**, respectively), and, in fact, requires a large quantity of enzyme. The high quantity of enzyme along with its overlapping absorbance precludes measurements at 232 nm and a determination of  $k_{\text{cat}}/K_{\text{m}}$  values. To enable a rough comparison of the relative activities of the Pp and Lc 4-OTs, the absorbance at 232 nm was monitored for a longer time period with identical amounts of dienol (150 μM, Figure S1 in Supporting Information File 1). In the presence of 150 μM of **5a**, the Pp 4-OT (2 μM) generates 120 μM of **9a** in 16 min, whereas the Lc 4-OT (35 μM) generates at least 90 μM of **9a** in 20 min. (In both experiments, the A<sub>232</sub> is outside the linear range so the amount of **9a** is likely being underestimated). For **5b**, the Pp 4-OT (2 μM) generates 33 μM of **9b** in 20 min, whereas the Lc 4-OT (2.3 μM) generates 11 μM of **9b** in 20 min. For **5c**, the Pp 4-OT (2 μM) gener-

**Table 5:** Kinetic parameters for Lc 4-OT using **5a–d**.<sup>a</sup>

| Reaction          |                    | $k_{\text{cat}}$ (s <sup>-1</sup> ) | $K_{\text{m}}$ (μM) | $k_{\text{cat}}/K_{\text{m}}$ (M <sup>-1</sup> s <sup>-1</sup> ) |
|-------------------|--------------------|-------------------------------------|---------------------|--|
|                   |                    |                                     |                     |  |
| <b>5a:</b> R = H  | <b>11a:</b> R = H  | 2.0 ± 0.3                           | 420 ± 89            | 4.8 ± 1.2 × 10 <sup>3</sup>                                      |
| <b>5b:</b> R = Cl | <b>11b:</b> R = Cl | 36 ± 6                              | 1400 ± 300          | 2.6 ± 0.7 × 10 <sup>4</sup>                                      |
| <b>5c:</b> R = Br | <b>11c:</b> R = Br | 13.2 ± 0.5                          | 290 ± 22            | 4.6 ± 0.4 × 10 <sup>4</sup>                                      |
| <b>5d:</b> R = F  | <b>11d:</b> R = F  | 25 ± 2                              | 850 ± 94            | 2.9 ± 0.4 × 10 <sup>4</sup>                                      |

<sup>a</sup>The steady-state kinetic parameters were determined under the conditions described in the text. Errors are standard deviations.



filter unit (3K membrane). This procedure typically yields  $\approx 8$  mg of 4-OT estimated to be  $\approx 95\%$  pure. A sample was analyzed by electrospray ionization mass spectrometry (ESIMS) to verify the molecular mass (6916 Da). In addition to this species (corresponding to the intact enzyme without the *N*-formylmethionine), there are five additional signals at 6475 Da, 6606 Da, 6634 Da, 7046 Da, and 7076 Da. These signals correspond to enzyme without the four C-terminal amino acids, the same enzyme with an N-terminal methionine, the same enzyme with an *N*-formylmethionine, the intact enzyme with an N-terminal methionine, and the intact enzyme with an *N*-formylmethionine [25].

### Synthesis of ethyl 2-fluorocrotonate and ethyl 2-bromocrotonate

Ethyl 2-fluorocrotonate was synthesized following published procedures [18]. Ethyl 2-bromocrotonate was synthesized following the protocol for the synthesis of ethyl 2-chlorocrotonate except that liquid bromine was added dropwise under argon in place of chlorine gas [11]. Accordingly, ethyl crotonate (15 g) was dissolved in  $\text{CH}_2\text{Cl}_2$  (100 mL), chilled in an ice bath, and a solution of bromine (21 g) dissolved in  $\text{CH}_2\text{Cl}_2$  (150 mL) was added over a period of 30 min. The solution was allowed to come to ambient temperature overnight. The solvent was removed under reduced pressure and the residue was distilled (3 torr, 79–81 °C) to leave a pale yellow liquid (29.7 g). The  $^1\text{H}$  and  $^{13}\text{C}$  NMR analysis indicated that the product formed was ethyl 2,3-dibromobutyrate. Subsequently, ethyl 2,3-dibromobutyrate was converted to ethyl 2-bromocrotonate following the procedure used to convert ethyl 2,3-dichlorobutyrate to ethyl 2-chlorocrotonate [11].

### Syntheses of 5-(halo)-2-hydroxyuconate (3c,d)

The syntheses of the 4*Z*-isomers of **3c** and **3d** (5-bromo- and 5-fluoro-, respectively) were based on the synthesis of (4*Z*)-**3b**, which followed the procedure used to produce 2-hydroxyuconate (**3a**) [8,11]. Sodium ethoxide was generated by allowing sodium metal (1 equiv, 26.2 and 17.3 g for **3c** and **3d**, respectively) to react completely with ethanol (50 mL), followed by the addition of toluene (300 mL) to the stirring mixture. The resulting solution was distilled (to remove water and ethanol) under an argon atmosphere until the temperature climbed above 80 °C. The anhydrous sodium ethoxide was chilled in an ice bath and diethyl oxalate (1 equiv, 6.5 g and 4.3 g for **3c** and **3d**, respectively) was added, followed by the addition of ethyl 2-bromo- or ethyl 2-fluorocrotonate [1 equiv, 6.7 g (42.4 mmol) and 4.4 g (27.9 mmol) for **3c** and **3d**, respectively]. The ethyl 2-halocrotonates consisted of an *E/Z* mixture with a predominance of the *E*-isomer. The reaction mixture was allowed to warm to ambient temperature. After being stirred at room tem-

perature for 72 h, the mixture was filtered and the precipitate washed with ether until the filtrate was clear. The precipitate was air-dried to yield the crude sodium salt of the diethyl ester of **3c** and **3d**, respectively. The free acid was prepared by alkaline hydrolysis of the diethyl ester and subsequent acidification as follows. The diethyl ester was suspended in water and chilled in an ice bath. Subsequently, a solution of 1 M NaOH (2.5 equiv) was added and the mixture stirred at ambient temperature for 16 h. The reaction mixture was filtered and the filtrate was adjusted to pH 1 by the addition of concentrated HCl. The precipitate was collected by filtration and crystallized in ethyl acetate (**3c**: 1.18 g and **3d**: 1.56 g). The  $^1\text{H}$ ,  $^{13}\text{C}$ , and  $^{19}\text{F}$  NMR data are presented in Supporting Information File 1.

### Syntheses of 5-(halo)-2-hydroxy-2,4-pentadienoate (5c,d)

The preparation of the 4*Z*-isomers of **5c** and **5d** was adapted from published procedures [10,11]. The diacid (200 mg, **3c** or **3d**) is combined with  $\approx 20$  mM  $\text{Na}_2\text{HPO}_4$  buffer (25 mL), and the pH was adjusted to 6.5–7.2 by the addition of aliquots of a 5 M NaOH solution. Adjustment of the pH results in the dissolution of the diacid. An aliquot ( $\approx 125$   $\mu\text{L}$ ) of a 1 M  $\text{MgCl}_2$  solution (for a final concentration of 3–5 mM) was then added to a suspension. For the preparation of **5c**, 4-OT is added to the diacid mixture and the mixture was incubated for 10 min. Subsequently, a sufficient quantity of 4-OD/E106QVPH (from *P. putida* mt-2) was added so that the reaction was complete within 20 min (monitored by UV spectroscopy). For the preparation of **5d**, an aliquot of 4-OT was added to the diacid mixture (which already contained 4-OD/E106QVPH and  $\text{MgCl}_2$ ) every min up to a 40 min period. The pH of both mixtures was adjusted to 1.8–2.0. The solution was extracted with ethyl acetate (3 $\times$ ), and the organic layers were pooled, dried over anhydrous  $\text{Na}_2\text{SO}_4$ , filtered, and evaporated to dryness at room temperature. The resulting solid was dissolved in  $\text{CH}_2\text{Cl}_2$ , and filtered through a nylon filter to remove the residual diacid. The organic layer was collected and evaporated to dryness at room temperature. The solid was dissolved in methanol, and the solution was passed through a nylon filter, collected, and diluted with ethyl acetate to azeotrope any water that is present in the methanol. The resulting solution was evaporated to dryness under reduced pressure at room temperature to yield the monoacid (**5c** or **5d**). Titration with hexanes yields a sticky yellow solid ( $\approx 100$  mg). The compounds are stored at  $-20$  °C. The  $^1\text{H}$ ,  $^{13}\text{C}$ , and  $^{19}\text{F}$  NMR data are presented in Supporting Information File 1.

### Equilibrium composition mixtures of 5b–d

In separate test tubes, **5b–d** (4 mg) was dissolved in dimethyl sulfoxide (DMSO)-*d*<sub>6</sub> (30  $\mu\text{L}$ ). The individual mixtures were

then added to 100 mM Na<sub>2</sub>HPO<sub>4</sub> buffer (600 μL, pH ≈9). The final pH ranged from 6.8–7.2. The Pp 4-OT (2 μL of a 43 mg/mL solution) was added to the mixture and the resulting mixture was placed in an NMR tube. The reactions were monitored by recording scans every 3 min until equilibrium had been reached (within 10 min). The spectra for the final mixtures were similar to those recorded for the samples that were allowed to equilibrate in buffer overnight. The approximate amounts of product in the mixtures were determined by integration of the signals, as described previously [15,26]. The C3 methylene protons show signals in the range of 3.39–3.53 ppm (2.41–2.53 ppm if hydrated) and the C5 methylene protons show signals in the range of 4.07–4.16 ppm. The <sup>1</sup>H NMR data are presented in Supporting Information File 1.

#### 4-OT-catalyzed ketonization of **5a–d**

The 4-OT-catalyzed ketonization of **5a–d** (Scheme 2) [27,28] was examined by following the decrease in absorbance at 280 nm ( $\epsilon = 8700 \text{ M}^{-1} \text{ cm}^{-1}$ ), 304 nm ( $\epsilon = 1300 \text{ M}^{-1} \text{ cm}^{-1}$ ), 304 nm ( $\epsilon = 2300 \text{ M}^{-1} \text{ cm}^{-1}$ ), and 284 nm ( $\epsilon = 4600 \text{ M}^{-1} \text{ cm}^{-1}$ ), respectively [9,22,23]. The decrease in absorbance corresponds to the ketonization of the dienol to the  $\beta,\gamma$ -unsaturated ketones (**11a–d**, respectively). These wavelengths and extinction coefficients were used to increase the concentration range and keep the collected data in the linear range of absorbance. The  $\lambda_{\text{max}}$  values for **5a–d** are 265 nm ( $\epsilon = 12700 \text{ M}^{-1} \text{ cm}^{-1}$ ), 278 nm ( $\epsilon = 14500 \text{ M}^{-1} \text{ cm}^{-1}$ ), 281 nm ( $\epsilon = 15100 \text{ M}^{-1} \text{ cm}^{-1}$ ), and 266 nm ( $\epsilon = 9400 \text{ M}^{-1} \text{ cm}^{-1}$ ), respectively. The reactions were carried out in 20 mM Na<sub>2</sub>HPO<sub>4</sub> buffer (1 mL, pH 7.3) containing Pp 4-OT (500 nM for **5a** and 66 nM for **5b–d**) or Lc 4-OT (3200 nM for **5a**, 500 nM for **5b** and **5d**, 1400 nM for **5c**). Assays were initiated by addition of varying amounts of **5a–d** (20–160 μM, 40–600 μM, 20–400 μM, and 20–300 μM, respectively) from stock solutions made up in ethanol (20, 40, 20, and 20 mM, respectively). The rapid non-enzymatic rates for **5a–c** were subtracted from the observed enzymatic rates. The non-enzymatic rate for **5d** was negligible. Data were collected every 0.5 s and the initial slope (resulting in the first 10 s of the reaction) was fit to a zero-order equation. The initial rates were determined in triplicate, averaged, plotted versus initial substrate concentration, and fit to determine  $k_{\text{cat}}$  and  $K_{\text{m}}$ . Nonlinear regression data analysis was performed using Mathematica (Wolfram Research, Inc., Mathematica, Version 8.0, Champaign, IL 2010).

The 4-OT-catalyzed conversion of dienols **5a–c** to their respective  $\alpha,\beta$ -unsaturated ketones **9a–c** (Scheme 2) was measured by following the increase in absorbance at 232 nm [9,10,14,16]. (There is no measureable increase in the absorbance at 232 nm for the reaction of 4-OT and **5d**, suggesting no detectable formation of **9d**.) Extinction coefficients were determined for **9b**

and **9c** following the protocol used to determine the extinction coefficient for **9a** [9]. Briefly, the absorbance of a known concentration of dienol (**5b** and **5c**) initially made up in ethanol and added to 20 mM NaH<sub>2</sub>PO<sub>4</sub> buffer (pH 7.3) was determined at 232 nm ( $\epsilon = 1700 \text{ M}^{-1} \text{ cm}^{-1}$  and  $1790 \text{ M}^{-1} \text{ cm}^{-1}$ , respectively). The solutions were then allowed to equilibrate in 20 mM NaH<sub>2</sub>PO<sub>4</sub> buffer (pH 7.3). The final absorbance at 232 nm was then corrected for the remaining dienol at equilibrium (15% and 9% for **5b** and **5c**, respectively) as well as the amount of conjugated ketone at equilibrium (39% and 61% for **9b** and **9c**, respectively). The ketonization reactions were carried out in 10 mM NaH<sub>2</sub>PO<sub>4</sub> buffer (1 mL, pH 7.3) containing 4 μM of Pp 4-OT. Assays were initiated by the addition of varying amounts of **5a**, **5b**, or **5c** (20–200 μM) from stock solutions made up in ethanol (20 mM). The increase in absorbance at 232 nm was assumed to be entirely due to the formation of the conjugated ketone ( $\epsilon = 5990 \text{ M}^{-1} \text{ cm}^{-1}$ ,  $11500 \text{ M}^{-1} \text{ cm}^{-1}$ , and  $9400 \text{ M}^{-1} \text{ cm}^{-1}$ , respectively). Data were collected every 0.5 s and the initial slope (5–20 s of the reaction) was fit to a zero-order equation. In the first 5 s of the reaction, the absorbance at 232 nm was still decreasing. Kinetic parameters were determined as described above.

The Lc 4-OT conversion of **5a–c** to the respective  $\alpha,\beta$ -unsaturated ketones **9a–c** was compared to the Pp 4-OT-catalyzed conversion by monitoring the spectral changes over 20 min. Aliquots of **5a–c**, made up as 20 mM stock solutions in ethanol, were added to 20 mM NaH<sub>2</sub>PO<sub>4</sub> buffer (1 mL, pH 7.3) with Pp 4-OT (2 μM) or Lc 4-OT (35 μM for **5a** or 2.3 μM for **5b,c**).

The 4-OT-catalyzed ketonization of **3b–d** (Scheme 2) was examined by following the decrease in absorbance at 284 nm ( $\epsilon = 9200 \text{ M}^{-1} \text{ cm}^{-1}$ ), 327 nm ( $\epsilon = 8400 \text{ M}^{-1} \text{ cm}^{-1}$ ), and 272 nm ( $\epsilon = 11300 \text{ M}^{-1} \text{ cm}^{-1}$ ), respectively. The decrease in absorbance corresponds to the ketonization of the dienol to the  $\beta,\gamma$ -unsaturated ketones (**3b–d** to **10b–d**, respectively). These wavelengths and extinction coefficients were used to increase the concentration range and keep the collected data in the linear range of absorbance. The  $\lambda_{\text{max}}$  values for **3b–d** are 304 nm ( $\epsilon = 14700 \text{ M}^{-1} \text{ cm}^{-1}$ ), 307 nm ( $\epsilon = 15100 \text{ M}^{-1} \text{ cm}^{-1}$ ), and 292 nm ( $\epsilon = 18300 \text{ M}^{-1} \text{ cm}^{-1}$ ), respectively. The reactions were carried out in 10 mM K<sub>2</sub>HPO<sub>4</sub> buffer (1 mL, pH 7.3) containing Pp 4-OT (12 nM for **3b** and **3c**, 1 nM for **3d**) or Lc 4-OT (8.75 nM for **3b**, 10.5 nM for **3c**, 1.75 nM for **3d**). Assays were initiated by addition of varying amounts of **3b–d** (15–120 μM, 16–125 μM, and 15–120 μM, respectively) from stock solutions made up in ethanol (20, 6.25, and 20 mM, respectively). The rapid non-enzymatic rates of **3b–d** were subtracted from the observed enzymatic rates. Data were collected every 0.5 s and the initial slope (resulting in the first 6 s of the reaction for **3b** and **3c**, the first 10 s of the reaction for **3d**) was fit to a zero-

order equation. Kinetic parameters were determined as described above.

### The 4-OT-catalyzed ketonization of **3a** to **4a**

The Pp and Lc 4-OT-catalyzed conversion of **3a** to the  $\alpha,\beta$ -unsaturated ketone, **4a** (Scheme 2) was measured by following the increase in absorbance at 236 nm [8]. The reactions were carried out in 10 mM  $\text{KH}_2\text{PO}_4$  buffer (1 mL, pH 7.3) containing 4 nM of Pp 4-OT or 1.75 nM of Lc 4-OT. Assays were initiated by the addition of varying amounts of **3a** (20–200  $\mu\text{M}$ ) from a stock solution made up in ethanol (20 mM). The increase in absorbance at 236 nm was assumed to be entirely due to the formation of the conjugated ketone ( $\epsilon = 6580 \text{ M}^{-1} \text{ cm}^{-1}$ ). Data were collected every 0.5 s and the initial slope (first 6 s of the reaction) was fit to a zero-order equation. Kinetic parameters were determined as described above. Both enzymes catalyze the conversion of **3b–d** (to **4b–d**), as determined by visual inspection, but kinetic parameters were not obtained.

## Supporting Information

### Supporting Information File 1

Analytical data.

[<http://www.beilstein-journals.org/bjoc/content/supplementary/1860-5397-13-101-S1.pdf>]

## Acknowledgements

The protein mass spectrometry analysis was conducted in the Institute for Cellular and Molecular Biology Protein and Metabolite Analysis Facility at the University of Texas at Austin. We thank Steve D. Sorey (Department of Chemistry, University of Texas at Austin) for his expert assistance in the acquisition of the  $^1\text{H}$  NMR spectra.

## References

- Parales, R. E.; Luu, R. A.; Hughes, J. G.; Ditty, J. L. *Curr. Opin. Biotechnol.* **2015**, *33*, 318–326. doi:10.1016/j.copbio.2015.03.017
- Huang, Z.; Ni, B.; Jiang, C.-Y.; Wu, Y.-F.; Parales, R. E.; Liu, S.-J. *Mol. Microbiol.* **2016**, *101*, 224–237. doi:10.1111/mmi.13385
- Wu, J.-f.; Jiang, C.-y.; Wang, B.-j.; Ma, Y.-f.; Liu, Z.-p.; Liu, S.-j. *Appl. Environ. Microbiol.* **2006**, *72*, 1759–1765. doi:10.1128/AEM.72.3.1759-1765.2006
- Bhowmik, S.; Horsman, G. P.; Bolin, J. T.; Eltis, L. D. *J. Biol. Chem.* **2007**, *282*, 36377–36385. doi:10.1074/jbc.M707035200
- Janssen, D. B.; Dinkla, I. J. T.; Poelarends, G. J.; Terpstra, P. *Environ. Microbiol.* **2005**, *7*, 1868–1882. doi:10.1111/j.1462-2920.2005.00966.x
- Dagley, S. Pathways for the utilization of organic growth substrates. In *The Bacteria: A Treatise on Structure and Function*; Ornston, L. N.; Sokatch, J. R., Eds.; Academic Press: New York, 1978; pp 305–388.
- Harayama, S.; Reki, M.; Ngai, K.-L.; Ornston, L. N. *J. Bacteriol.* **1989**, *171*, 6251–6258. doi:10.1128/jb.171.11.6251-6258.1989
- Whitman, C. P.; Aird, B. A.; Gillespie, W. R.; Stolowich, N. J. *J. Am. Chem. Soc.* **1991**, *113*, 3154–3162. doi:10.1021/ja00008a052
- Lian, H.; Whitman, C. P. *J. Am. Chem. Soc.* **1994**, *116*, 10403–10411. doi:10.1021/ja00102a007
- Stanley, T. M.; Johnson, W. H., Jr.; Burks, E. A.; Whitman, C. P.; Hwang, C.-C.; Cook, P. F. *Biochemistry* **2000**, *39*, 718–726. doi:10.1021/bi9918902
- Johnson, W. H., Jr.; Stack, T. M. M.; Taylor, S. M.; Burks, E. A.; Whitman, C. P. *Biochemistry* **2016**, *55*, 4055–4064. doi:10.1021/acs.biochem.6b00552
- Manjasetty, B. A.; Powlowski, J.; Vrieling, A. *Proc. Natl. Acad. Sci. U. S. A.* **2003**, *100*, 6992–6997. doi:10.1073/pnas.1236794100
- Zhang, Y.; Wu, J.-F.; Zeyer, J.; Meng, B.; Liu, L.; Jiang, C.-Y.; Liu, S.-Q.; Liu, S.-J. *Biodegradation* **2009**, *20*, 55–66. doi:10.1007/s10532-008-9199-x
- Burks, E. A.; Yan, W.; Johnson, W. H., Jr.; Li, W.; Schroeder, G. K.; Min, C.; Gerrata, B.; Zhang, Y.; Whitman, C. P. *Biochemistry* **2011**, *50*, 7600–7611. doi:10.1021/bi200947w
- Huddleston, J. P.; Johnson, W. H., Jr.; Schroeder, G. K.; Whitman, C. P. *Biochemistry* **2015**, *54*, 3009–3023. doi:10.1021/acs.biochem.5b00240
- Lian, H.; Czerwinski, R. M.; Stanley, T. M.; Johnson, W. H., Jr.; Watson, R. J.; Whitman, C. P. *Bioorg. Chem.* **1998**, *26*, 141–156. doi:10.1006/bioo.1998.1095
- Lian, H.; Whitman, C. P. *J. Am. Chem. Soc.* **1993**, *115*, 7978–7984. doi:10.1021/ja00071a007
- Clemenceau, D.; Cousseau, J. *Tetrahedron Lett.* **1993**, *34*, 6903–6906. doi:10.1016/S0040-4039(00)91826-4
- Burks, E. A.; Fleming, C. D.; Mesecar, A. D.; Whitman, C. P.; Pegan, S. D. *Biochemistry* **2010**, *49*, 5016–5027. doi:10.1021/bi100502z
- Poelarends, G. J.; Almrud, J. J.; Serrano, H.; Darty, J. E.; Johnson, W. H., Jr.; Hackert, M. L.; Whitman, C. P. *Biochemistry* **2006**, *45*, 7700–7708. doi:10.1021/bi0600603
- Wang, S. C.; Person, M. D.; Johnson, W. H., Jr.; Whitman, C. P. *Biochemistry* **2003**, *42*, 8762–8773. doi:10.1021/bi034598+
- Waddell, W. J. *J. Lab. Clin. Med.* **1956**, *48*, 311–314.
- Schägger, H.; von Jagow, G. *Anal. Biochem.* **1987**, *166*, 368–379. doi:10.1016/0003-2697(87)90587-2
- Laemmli, U. K. *Nature* **1970**, *227*, 680–685. doi:10.1038/227680a0
- Hirel, P.-H.; Schmitter, J.-M.; Dessen, P.; Fayat, G.; Blanquet, S. *Proc. Natl. Acad. Sci. U. S. A.* **1989**, *86*, 8247–8251. doi:10.1073/pnas.86.21.8247
- Wang, S. C.; Johnson, W. H., Jr.; Whitman, C. P. *J. Am. Chem. Soc.* **2003**, *125*, 14282–14283. doi:10.1021/ja0370948
- Strenda DB data set. doi:10.22011/strenda\_db.OPC8OQ
- Strenda DB data set. doi:10.22011/strenda\_db.XG8UGZ

## License and Terms

This is an Open Access article under the terms of the Creative Commons Attribution License (<http://creativecommons.org/licenses/by/4.0>), which permits unrestricted use, distribution, and reproduction in any medium, provided the original work is properly cited.

The license is subject to the *Beilstein Journal of Organic Chemistry* terms and conditions: (<http://www.beilstein-journals.org/bjoc>)

The definitive version of this article is the electronic one which can be found at:  
[doi:10.3762/bjoc.13.101](https://doi.org/10.3762/bjoc.13.101)